

ENIGMATIC CARBON-13-RICH MATERIALS IN MICROMETEORITE TAM19B-7. M. Bose^{1*}, V. Froh^{1,2*}, and M. D. Suttle^{3,4}, ¹School of Earth and Space Exploration, Arizona State University (Maitrayee.Bose@asu.edu). ²School of Molecular Sciences, Arizona State University. ³Natural History Museum, London. ⁴Dipartimento di Scienze della Terra, Università di Pisa. *Center for Isotope Analysis.

Introduction: TAM19B-7 is one of the largest unmelted, fine-grained micrometeorite (FgMM) discovered. This micrometeorite was recovered from loose sediment traps at Miller Butte within the Transantarctic Mountains (TAM), Antarctica [1] and subsequently analyzed to resolve its parent body [2] and atmospheric entry [3] history.

Most micrometeorites (50–80%) in our collection originate from CM/CR carbonaceous chondrite parent bodies [3–5], and ~30% of measured samples have oxygen isotope compositions that relate them to ordinary chondrites or other, as yet, unsampled parent bodies [6]. The oxygen isotope composition of TAM19B-7 plots above the Terrestrial Fractionation Line (TFL) but due to terrestrial weathering have been drawn to lighter $\delta^{18}\text{O}$ values ($\Delta^{17}\text{O} = 0.5\text{‰}$, $\delta^{18}\text{O} = 1\text{‰}$). TAM19B-7's composition above the TFL combined with its hydrated carbonaceous chondrite texture limits the number of possible parent bodies significantly. This micrometeorite most likely derives from the enigmatic “group 4” population [6] or a member of the CI/CY groups [7]. The “group 4” particles are a new class not represented among meteorites with currently unknown affinities, and we argue that TAM19B-7 provides evidence of the existence of an intensely hydrated carbonaceous chondrite object in the main belt.

FgMMs with relict textures and anhydrous matrices probably experienced minimum peak temperatures of $>700^\circ\text{C}$ and $<\sim 1350^\circ\text{C}$ [8]. However, carbonaceous and organic phases, which appear in Raman spectra as ‘G’ and ‘D’ bands are preserved in TAM19B-7 [9], which suggests only modest heating, probably below 800°C [10] experienced by this particle. The carbon isotopes in insoluble organic matter (IOM) in carbonaceous chondrites have previously been characterized [11], while that in micrometeorites is unknown. Here we report the carbon isotopic compositions of two fragments in the micrometeorite TAM19B-7.

Methods: The original TAM19B-7 particle was imaged as a loose particle, set in resin, sectioned and polished for documentation and preliminary analysis using SEM-EDS. The particle was pulled out of the resin mechanically and the main mass analyzed for oxygen isotopes using laser fluorination mass spectrometry at Open University.

The remaining smaller fragments were re-embedded in resin and the carbon isotopic composi-

tions were acquired in the fine-grained and dark materials, using the NanoSIMS 50L at Arizona State University. We measured carbon isotopes in two fragments (Figure 1) in the epoxy disc. We used a 5 pA (D1-3) Cs^+ ion beam to raster $5 \times 5\ \mu\text{m}^2$ area and measured $^{12,13}\text{C}$, ^{16}O , $^{12}\text{C}^{14}\text{N}$, $^{12}\text{C}^{15}\text{N}$, and ^{28}Si simultaneously at high mass-resolving power to resolve interferences ($\sim 12,000$ Cameca Mass Resolving Power with ES-3 and AS-3). A 20 pA current was used to presputter a larger $10 \times 10\ \mu\text{m}^2$ area to remove the gold coat and implant the sample with Cs. We don't report the nitrogen isotope compositions of the fragments because the nitrogen counts were too low. The standard used for these measurements was cyanoacrylate ‘Crazy-Glue’ with known carbon and nitrogen isotope compositions [12]. The fragments are porous and were mounted in epoxy; therefore, we measured several spots on the epoxy to measure its carbon isotopic composition, and distinguish it from the organic materials in the fragments.

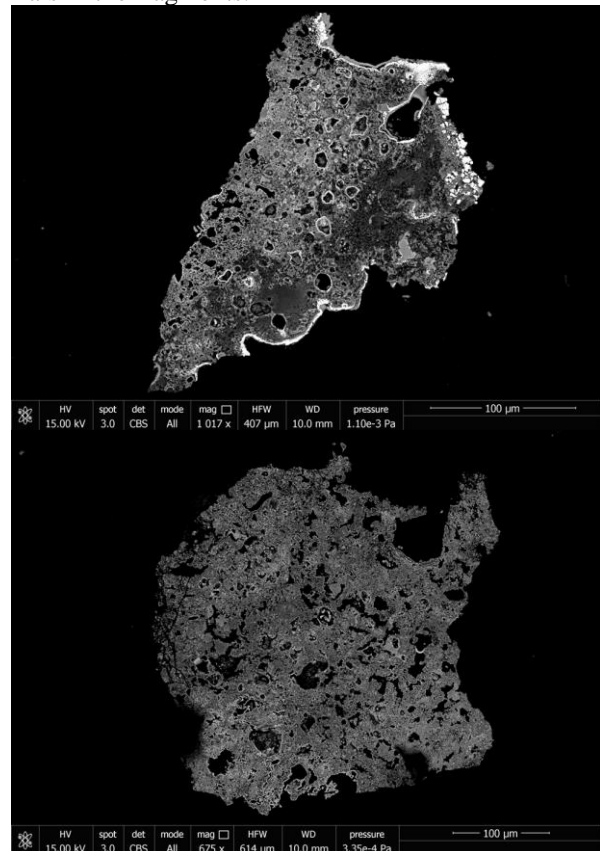


Figure 1. Back-scattered electron image of the two fragments in TAM19B-7 that were measured.

Results: Out of 7 measured areas in the two fragments, two exhibit ^{13}C enrichments ($\delta^{13}\text{C} = 95\text{--}111\text{‰}$; Figure 2). Smaller ^{13}C enrichments ($\delta^{13}\text{C} = 36\text{--}38\text{‰}$) were observed in several spots, but their values are also within the range measured for the epoxy and thus could be either parent body or terrestrial artefacts. Further measurements using Raman spectroscopic mapping will discriminate these possibilities.

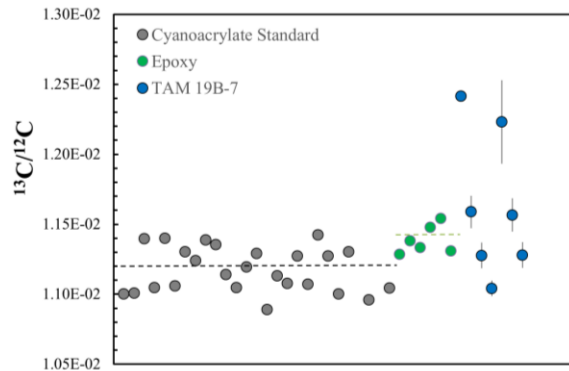


Figure 2. Carbon isotope compositions measured in several areas in two fragments in TAM19B-7, along with the cyanoacrylate standard and epoxy in which the fragments were mounted. Two areas on the fragments probably containing carbonate grains show ^{13}C excesses. 1σ error bar = standard error are shown.

Discussion: Possible candidates for the carrier phases of the ^{13}C -rich areas are presolar carbonaceous phases; macromolecular matter in meteorites or IOM; or carbonate minerals.

Presolar SiC and graphite phases can vary in size from 100s of nm to 10s of μm ; $^{12}\text{C}/^{13}\text{C}$ ratios in these grains spans a large range, 10–10,000 [13]. Moderate enrichments ($\delta^{13}\text{C} \sim 480\text{‰}$) in (say) a 1 μm -sized presolar grain present in the region of interest and signal dilution from the micrometeorite's fine-grained matrix can explain the observed ^{13}C -rich compositions in TAM19B-7. However, the abundance of presolar grains decrease considerably due to aqueous processing [e.g., 8]. TAM19B-7 experienced intense aqueous alteration [2] and so the probability of presolar grain survival is extremely low.

Alternatively, disordered carbonaceous matter is observed in all fine-grained unmelted and almost all scoriaceous particles [10], suggesting this form of carbon is more resistant to atmospheric entry than carbonates. The Raman data from TAM19B-7 also confirms that heated but disordered carbonaceous matter is present in TAM19B-7 [3]. The carbon isotopic composition of meteoritic IOM in CM and heated CMs ranges from -8 to -20 ‰ [11], in contrast to the ^{13}C -rich compositions measured for TAM19B-7 (Fig-

ure 2). Carbonaceous chondrites also have ^{13}C -anomalous hotspots but they are usually rare and small (100–200 nm) in magnitude [15–16]. Therefore, based on the carbon isotopic compositions alone, meteoritic IOM-like material is the least likely carrier phase.

Carbonates in CM carbonaceous chondrites show ^{13}C enrichments of up to 80 ‰ [17–18]. The calcite grain sizes vary from less than 5 μm to $\sim 100\text{ }\mu\text{m}$ across while the dolomite grains can be small (<3 μm). Considering that we were measuring $5 \times 5\text{ }\mu\text{m}^2$ areas and have observed ^{13}C enrichments comparable to that seen in carbonates, it is possible that the measured ^{13}C -rich areas contain calcite or dolomite grains. Carbonates in the matrices of micrometeorites are argued to be rare and to *not* survive atmospheric entry because temperatures for thermal decomposition are as low as 400°C [19]. However, a 10 μm magnetite-dolomite assemblage was recently reported in a hydrated FgMM, 03-36-46 from Concordia [20] suggesting similar secondary alteration assemblages could be present in TAM19B-7.

Future Work: We plan to measure additional regions in TAM19B-7 and correlate ^{13}C enrichments with their associated phases. We will first use Raman maps, to avoid damaging potential carbonate carrier phases, which are known to be beam sensitive. Later we will acquire higher resolution BSE and EDX maps on each of the $5 \times 5\text{ }\mu\text{m}$ regions (previously) measured for carbon isotopes.

Acknowledgement: We would like to thank PNRA - Meteoriti Antartiche project and Dr. Ziliang Jin for NanoSIMS assistance.

References: [1] Suavet C. et al. (2009) *Pol. Sci.*, 3, 100–109. [2] Suttle M. D. (2019) *GCA*, 245, 352–373. [3] Suttle M. D. (2019) *MAPS*, 54, 503–520. [4] Taylor S. et al. (2012) *MAPS*, 47, 550–564. [5] Corder C. and Folco L. (2014) *GCA*, 146, 18–26. [6] Suavet C. et al. (2010) *EPSL*, 293, 313–320. [7] King A. et al. (2019) *Geochem.*, 79, 125531. [8] Toppani A. et al. (2001) *MAPS*, 36, 1377–1396. [9] Suttle M. D. et al. (2017) *GCA*, 206, 112–136. [10] Dobrică E. et al. (2011) *MAPS*, 46, 1363–1375. [11] Alexander C. M. O'D. et al. (2007) *GCA*, 71, 4380–4430. [12] Bose M. et al. (2014) *EPSL*, 399, 128–138. [13] Zinner E. (2013) [14] Trigo-Rodriguez J.M. and Blum J. (2009) *Pub. Astro. Soc. Austr.*, 26, 289–296. [15] Floss C. and Stadermann F. (2009) *GCA*, 73, 2415–2440. [16] Bose M. et al (2012) *GCA*, 93, 77–101. [17] Tyra M. et al (2016) *GCA*, 175, 195–207. [18] Telus M. et al (2019) *GCA*, 260, 275–291. [19] Nozaki W. et al (2010) *MAPS*, 41, 1095–1114. [20] Ogliore R.C. et al (2019) *LPSC 50* (Abstract #2778).